A New Source of the Slow Solar Wind

Bala Poduval and Xue Pu Zhao

Hansen Experimental Physics Laboratory, Stanford University, Stanford, CA 94305 USA

Abstract

Slow solar wind has been found to exhibit a high level of variability and the source is still unclear. Helmet streamers underneath the base of the heliospheric current sheet has been suggested to be the source of slow solar wind, though low latitude coronal holes could be another source. It has been shown recently that the helmet streamers occur between coronal holes of opposite polarity as well as between coronal holes of like polarity. The former is called the bipolar closed field regions and the latter unipolar closed field regions (Zhao and Webb, 2003). We investigate the association of slow solar wind observed by WIND, ACE and IPS with unipolar closed field regions.

Introduction

There are two distinct components in the solar wind in the heliosphere; the fast with speed above 450 km s^{-1} and the slow, with velocity less than 450 km s^{-1}. The fast wind originates from coronal holes where the magnetic field lines are open while the slow wind is expected to come from closed field regions. However, the source of slow wind is still not clearly understood and is now a widely studied topic. Wang (1994) has identified two sources of slow solar wind, the boundaries of the large polar coronal holes and small coronal holes. His analysis is based on flux divergence and associated solar wind speed. Accoring to this theory, these two sources of slow solar wind are associated with rapidly diverging magnetic field. The former is responsible for slow solar wind found near the heliospheric current sheet and the latter is give rise to slow solar wind observed near solar maximum. In another study, Wang et al., (1998) identified the closed coronal loops or the helmet streamer, and the rapidly diverging open flux tubes rooted inside the coronal holes as the two sources of slow solar wind. Neugebauer et al., (1998) have also identified intermediate and slow solar wind originatiing from small coronal holes at low latitudes.

Lundstedt (1989) has carried out a study of the coronal sources of slow solar wind by mapping the solar wind observed at 1 AU back to the source surface. They used 3-hr averages of solar wind speed and selected those events whose velocity remained below 350 km s^{-1} for a minimum of 4 days. In their study, they found that very low hourly values of temperature, $\sim 5 \times 10^3$ K, and density, 5.2 ions/cm^{-1}, while solar wind speed was moderately low, $\sim$ 311 km s^{-1}. They grouped the source locations as 'along the neutral line', 'crossing the neutral line', and 'inside a warp'. They identified 25 events of which 4 were 'along the neutral line', another 4 were 'inside a warp' and the remaining 17 were found to be 'crossing the neutral line'. They concluded by noting that the slow wind found 'inside a warp' was quite unexpected since slow wind was expected to originate in a region of closed magnetic field.

The slow solar wind observed in the synoptic maps on the source surface deduced from Interplanetary Scintillation (IPS) techniques were used by Ohmi et al., al (2004) to infer the source of slow solar wind. They found that the slow solar wind originates from an equatorial coronal hole near active regions and also from a polar coronal hole that was about to disappear at solar maximum (see also Ohmi, 2003). The slow wind from the equatorial coronal hole had properties similar to that of fast wind from a large coronal hole, i.e., they had uniform magnetic polarity, the ratio of alpha paricles to proton was as large as fast wind, whereas, variances of density, velocity and helium abundances were as small as fast wind from a large coronal hole. On the other hand, properties like density and the ion freez-in temperature were as large as the slow solar wind from the heliospheric plasma sheet.

We present the preliminary results of a study of the coronal sources of slow solar wind by mapping the solar wind observed near the Earth back to the source surface at 2.5 $R_\odot$. The source regions were identified using a potential field source surface (PFSS) model of the corona.

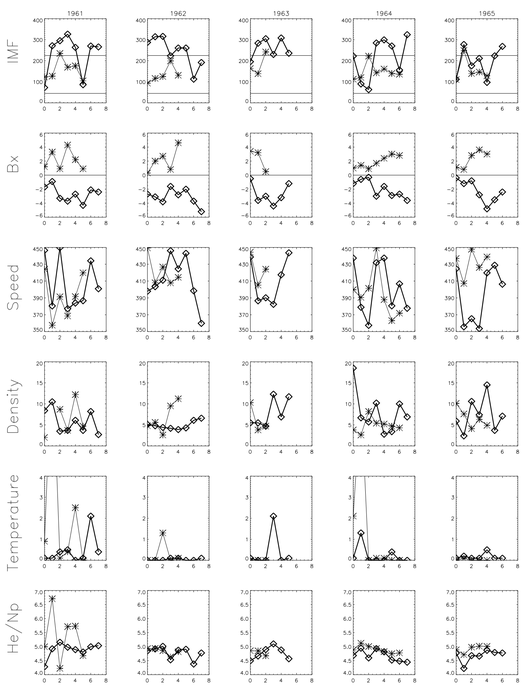

Figure 1. The solar wind properties for the medium speed (between 350 and 450 km s^{-1}) wind, for CRs 1961–1965. Panel 1: IMF, longitude of average field vector. A value between 45 and 225 is considered positive and above 225 is negative. Panel 2: Bx, Panel 3: Solar wind speed, Panel 4: density, Panel 5: temperature, Panel 6: ratio of helium to proton.

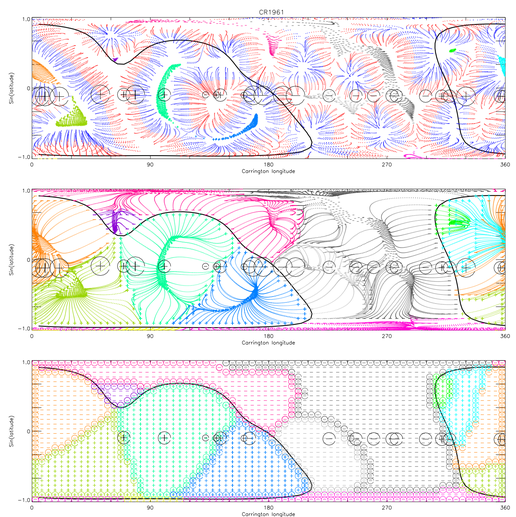

Figure 2. The mapping of open field regions using the PFSS model during solar maximum: CR1961. Top panel: coronal open (colored dotted areas) and closed (areas consisting of blue-red field lines) field regions below 1.25 $R_\odot$. Middle panel: radial extension of the boundaries of open field regions to the source surface at 2.5 $R_\odot$. Bottom panel: two kinds of boundary layers between open field regions at the source surface; bipolar (coincident with the black neutral line) and unipolar boundary layers. The solar wind observed near the Earth during the same period in different speed range as described in the text are superposed in each panel.

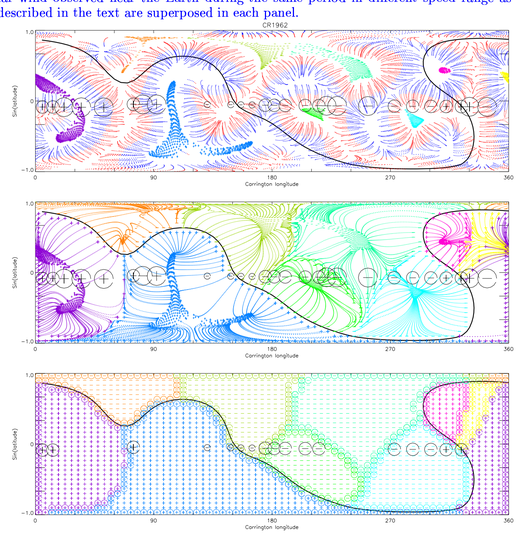

Figure 3. Same as Figure 2, but for CR 1962.

Potential Field Source Surface Model

The coronal magnetic field can be computed from the observed photospheric magnetic field by solving the LaPlace's equation, based on the assumptions that the coronal field is a potential field since the currents carried by plasma are negligible and the field at the source surface, at 2.5 $R_\odot$, is purely radial. A coronal model of this kind is called Potential Field Source Surface (PFSS) model and has been useful in predicting the observed structures, though discrepancies do exist. The PFSS model was first put forth by Schatten et al., (1969) and independently, by Altschuler and Newkirk (1969). The model has a few free parameters: height of source surface: 2.5 or 2.35 $R_\odot$, the radius of the inner surface: 1.0 $R_\odot$ or slightly different, the number of multipole components included in the spherical harmonic expansion of fields, represented by N_{max}.

Data and Procedure

Photospheric magnetic field data: from Kitt Peak (KPK). Using PFSS model of the corona, the open field regions were traced to the photosphere and the foot point locations were obtained. Also, the closed field regions were marked and the boundary between open field regions were identified.

Solar wind data: OMNI data corresponding to Carrington rotations 1961-1965, during solar maximum in 2000. (http://nssdc.gsfc.nasa.gov/omniweb/)

In order to identify the source regions, the solar wind observed in the heliosphere is mapped back to the source surface using the following set of equations:

$$\theta_{ss} = \theta_E$$
$$\phi_{ss} = \phi_E + \frac{\omega R_E}{V} \qquad (1)$$

where, θ_{ss} and ϕ_{ss} are heliographic latitude and Carrington longitudes of the source of solar wind at the source surface, θ_E and ϕ_E are the heliographic latitude and Carrington longitudes at distance R_E from Sun, ω, the angular speed of solar rotation and V, is the solar wind speed. In this study, we used the daily averaged values of the observed values of solar wind (Poduval and Zhao, 2004).

Two kinds of closed field regions

Hundhausen (1972; Figure 7.1) suggested that there exists two kinds of magnetid field topologies beneath a helmet streamer. One is the typical single arcade and the other, two arcades. We call the former *bipolar* helmet streamer that occurs between coronal holes (open field regions) of opposite magnetic polarity, and the latter, *unipolar* helmet streamer, occurring between open field regions of the same plarity (Zhao and Webb, 2003). Near solar minimum, the helmet streamers are found between the northern and southern polar coronal holes with opposite magnetic polarity, forming the bipolar helmet streamer belt in the corona, the base of the heliospheric current sheet (HCS). As solar activity increases coronal holes begin to appear at low latitudes as well and the rate of occurrence of unipolar helmet streamers between coronal holes of the same polarity increases (See Zhao and Webb, 2003 for details).

Figure 1 shows the properties of solar wind of medium speed (in the range 350–450 km s^{-1}) for all the Carrington rotations CR1961–1965. In Panels 1 and 2, the longitude of the average field vector of the IMF and Bx are plotted. The speed, number density and temperature are plotted in Panels 3-5. The ratio of alpha particles to protons is plotted in Panel 6.

Figures 2–6 depict open and closed field regions near sunspot maximum CRs 1961–1965 (April–August, 2000) as well as the unipolar and bipolar boundary layers of open field regions at the source surface.

Top panels: Distribution of the two kinds of closed field regions. The open field regions are shown as coloured patches of irregular shapes. The magnetic polarity of each open field region can be found from the area with same color at the source surface in the bottom panel. Magnetic polarities away from the Sun are maked by '+' and those toward the Sun are shown by '-' symbols. Closed field regions away from the neutral lines occur between open field regions of the same polarity. Examples: those between the orange and pale green open field regions between $0 - 90°$ longitude; between the pale green and blue open field regions right next to it in Figure 2. Superposed are the solar wind speed observed near the Earth available from OMNI data center, during the same period. Three ranges of speed, identified as, below 350 km s^{-1} between 350 and 450 km s^{-1} and above 450 km s^{-1} , are represented by open circles of differing sizes, small, medium and large, respectively. Within each of these circles are the magnetic polarity associated with each solar wind, positive (+) and negative (-).

Middle panel: radial variation of the boundary of the open field regions from 1.0 to 2.5 solar radii. Solar wind speed in the three ranges described in the previos paragraph are also superposed.

Bottom panel: boundary layers of open field regions at 2.5 solar radii. In addition to the bipolar boundary layer between opposite-polarity open field regions, which is the magnetic neutral line shown as thick black line, there are several unipolar boundary layers between open field regions of the same polarity. Examples are given in the preceeding paragraph. Superposed are the solar wind speed in the ranges, below 350 km s^{-1} and between 350 and 450 km s^{-1} represented by small and medium circles. The associated polarity is also marked as described above.

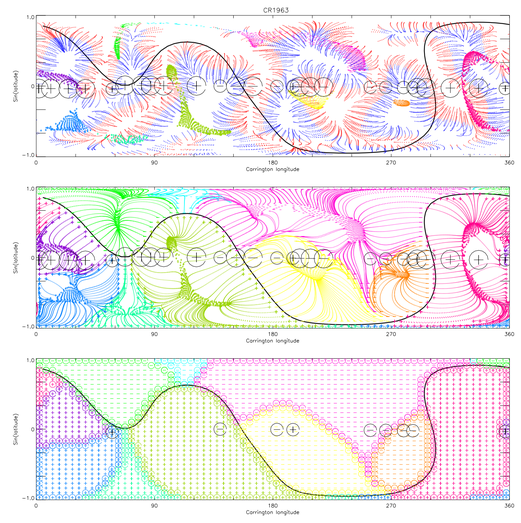

Figure 4. Same as Figure 2 but for CR 1963.

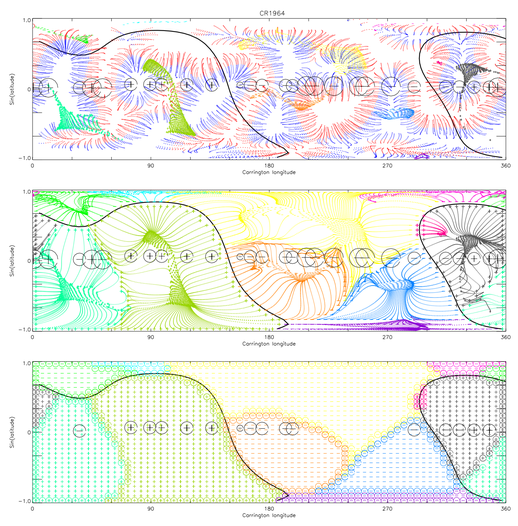

Figure 5. Same as Figure 2 but for CR 1964.

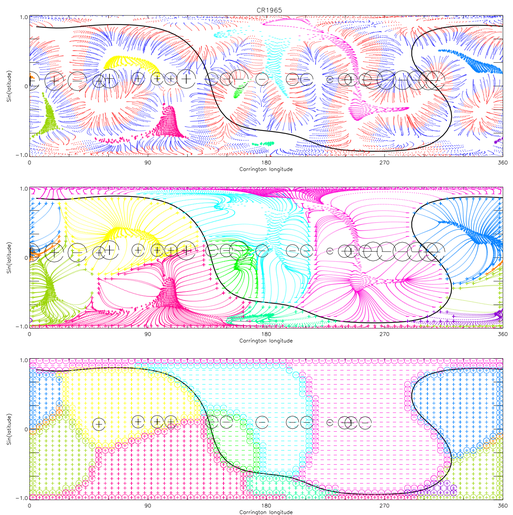

Figure 6. Same as Figure 2 but for CR 1965.

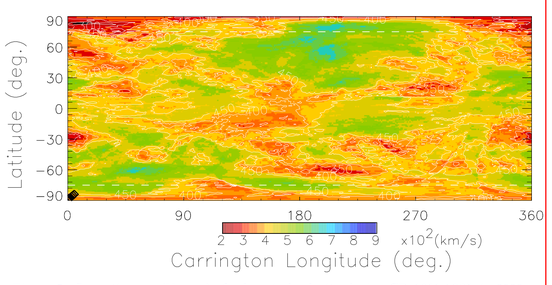

Figure 7. Synoptic map (V-map) of solar wind velocity during CRs1961-1965, in 2000, after applying the technique of tomography.

Discussion and Conclusion

From the present analysis, we find that the very slow solar wind (< 350 km s^{-1}) occur mostly on or close to the magnetic neutral line or HCS, which is the boundary between open field regions of opposite polarity. There are several occassions when solar wind of medium speed (between 350 and 450 km s^{-1}) were found to be originating from the boundary of open field regions of the same poarity, unipolar boundary layer. In most cases the magnetic field polarity associated with the observed solar wind was found to be the same as that of the unipolar open field regions. It has to be mentioned that there are exceptions to this which may be due to the imperfect inverse mapping of solar wind to the source surface or due to the presence of transients.

Further, referring to the middle panel in Figures 2–6, there are cases when slow wind are traced to the centre of a unipolar open field region as well as high speed wind occurring near the unipolar boundary layer. This is unexpected. During solar maximum, the systematic increase in the solar wind speed with latitude seen near the Earth during solar minimum is absent and the slow and fast solar wind occur everywhere. Also, it is to be noted that during the period of study, CRs1961–1965, the very high speed solar wind were absent as seen from the V-map (Figure 7) deduced using the IPS–tomography technique of STELab, Nagoya, Japan. Though, these discrepancies need to be investigated further, which is currently underway, the boundary between unipolar open field regions are strongly considered to be source of medium speed $\sim$ 450 km s^{-1} solar wind.

References

Altschuler, M. D. and G. Newkirk, Jr., *Solar Phys.*, **9**, 131, 1969.

Hundhausen, A. J., Coronal Expansion and Solar Wind, Phys. Chem. Space, vol. 5, Springer-Verlag, New York, 1972.

Lundstedt, H., *Solar Phys.*, **123**, 177–183, 1989.

Neugebauer et al., *Journal Geophys. Res.*, **103**, 14587–14599, 1998.

Ohmi, T., The Origin of the low–speed solar wind, Ph. D. Thesis, Nagoya University, Japan.

Ohmi, T., M. Kojima, M. Tokumaru, K. Fujiki, K. Hakamada, *Advances in Space Research*, **33**, 689–695, 2004.

Poduval, B., X.-P. Zhao, *Journal Geophys. Res.*, **109**, A08102, doi:10.1029/2004JA010384, 2004.

Schatten, K. J., W. Wilcox, and N. F. Ness, *Solar Phys.*, **6**, 442, 1969.

Wang, Y.-M., *Astrophys. J.*, **437**, L67–L70, 1994.

Wang, Y.-M., N. R. Sheeley, Jr., Walters, J.H., Brueckner, G. E., Howard, R. A., Michels, D. J., Lamy, P. L., Schwenn, R., and Simnett, G.M., *Astrophys. J.*, **498**, L165–L168, 1998.

Zhao, X.-P., and D. F. Webb, *Journal Geophys. Res.*, **108**, 1234, doi:10.1029/2002JA009606, 2003.